Analysis of MIMO Spatial Multiplexing under Limited Feedback

A Project Report

submitted by

A.SAIVENKATESH

in partial fulfilment of the requirements

for the award of the degree of

BACHELOR AND MASTER OF TECHNOLOGY

DEPARTMENT OF ELECTRICAL ENGINEERING
INDIAN INSTITUTE OF TECHNOLOGY MADRAS.

May 2014

THESIS CERTIFICATE

This is to certify that the thesis titled **Analysis of MIMO Spatial Multiplexing under Limited Feedback**, submitted by **A. Saivenkatesh**, to the Indian Institute of Technology, Madras, for the award of the degree of **Bachelor and Master of Technology**, is a bona fide record of the research work done by him under my supervision. The contents of this thesis, in full or in parts, have not been submitted to any other Institute or University for the award of any degree or diploma.

Prof.R.David Koilpillai
Research Guide
Professor
Dept. of Electrical Engineering
IIT Madras, 600 036

Place: Chennai

Date: 5^{th} May 2014

ACKNOWLEDGEMENTS

I would like to thank my guide Prof.R.David Koilpillai for his support and assistance through my project. His guidance has been essential for the project. I would like to thank all my professors and friends for having assisted me through the dual degree course. I am grateful to Ravi Kiran, Ankit Behura, Chitra K R, Sai Shankar, Bharadwaj and Anup for their inputs during the course of my project. I would also like to thank Dr. Klutto, CeWit for his assistance on understanding MIMO spatial multiplexing. Finally, I thank my parents for their sacrifices and support throughout.

ABSTRACT

KEYWORDS: MIMO; Spatial Multiplexing; GTD; GMD; Bit Loading; Precoder; Codebook Selection;Grassman Codebook

Many current wireless technologies, including 3G and 4G standards, use MIMO Spatial Multiplexing to achieve higher data rates. In this report MIMO Transceiver algorithms involving Generalized triangular decomposition (GTD), Geometric Mean Decomposition (GMD) and Singular Value Decomposition (SVD) are studied under limited feedback scenarios using the LTE precoder codebooks and Grassman codebooks. Key results of the thesis include optimal bit allocation under limited feedback and analysis of noise conditioning by precoding. A sub-optimal codebook size reduction algorithm is also introduced to achieve flexible codebook sizes and reducing computational complexity, it is shown that sub-optimal reduction often leads to only a marginal degradation in BER. This codebook reduction maybe used in good channel conditions to save valuable feedback bits and computation. Also the possibility of channel estimation errors being masked by the precoder quantization is studied.

TABLE OF CONTENTS

LIST OF TABLES

LIST OF FIGURES

ABBREVIATIONS

AWGN	Additive White Gaussian Noise
BA	Bit Allocation
BER	Bit Error Rate
BLER	Block Error Rate
CSIR	Channel State Information at the Receiver
CSIT	Channel State Information at the Transmitter
CQI	Channel Quality Information
DFE	Decision Feedback Equalizer
EESM	Exponential Effective Signal to Noise Ratio Mapping
GMD	Geometric Mean Decomposition
GTD	Generalised Triangular Decomposition
IID	Independent and Identically Distributed
LTE	Long Term Evolution
MIESM	Mutual Information based Effective Signal to Noise Ratio Mapping
MIMO	Multiple Input Multiple Output
MMSE	Minimum Mean Square Error
PMI	Precoder Matrix Indicator
QAM	Quadrature Amplitude Modulation
QPSK	Quadrature Phase Shift Keying
RI	Rank Index
Rx	Receiver
SNR	Signal to Noise Ratio
SVD	Singular Value Decompostion
Tx	Transmitter
ZF	Zero Forcing

NOTATION

N_r	No of receiver antennas
N_t	No. of transmitter antennas
H	Channel Matrix
b_k	Number bits allocated to the k^{th} stream of MIMO communicatio system
b	Total number bits transmitted across the MIMO transceiver
s	Transmitted symbol vector
σ_i	i^{th} singular value of the matrix under consideration
P_k	Power to be used on the k^{th} stream
$\mathbf{C_n}$	Covariance of noise vector $\mathbf{n}$
σ_n	Noise variance

CHAPTER 1

Introduction

Wireless communication poses multiple impairments and challenges caused by additive noise, fading and Doppler effects. In the quest to achieve better performance and near Shannon capacity various methods such as error control codes have been used by wireless technologies(Goldsmith (2005)). Multiple transmit or receive antennas have been used to achieve diversity gain. MIMO allows for the use of multiple transmit and receive antennas in wireless communication systems. Use of multiple antennas allows for the utilization of the array gain, spatial diversity, spatial multiplexing gain, co-operative diversity gain, beamforming etc(Mietzner *et al.* (2009)) provides a comprehensive survey of MIMO applcations. MIMO systems are widely in use in most of the current wireless standards, including IEEE 802.11n, 3GPP LTE and WiMax ,either with the aim of reducing the bit error rate using spatial diversity or to increase the rate of transmission using spatial multiplexing or combination of both. While there are many MIMO modes in practice (the MIMO modes utilised by LTE are mentioned in Appendix A), in this thesis we are looking at possible improvements in the spatial multiplexing mode. This report includes the analysis on spatial multiplexing and provides some interesting and novel properties.

1.1 MIMO Spatial Multiplexing

Spatial multiplexing is the technique using MIMO wireless transmission to transmit multiple signals in parallel. If there are N_r receive antennas and N_t transmit antennas then a maximum of $N = min(N_r, N_t)$ signals can be transmitted without any additional use of power. Each of these independent signals are refered to as data streams. The proof for the N fold increase in capacity was provided by (Telatar (1999)).The N fold increase in spectral efficiency is usually limited by the spatial correlation between the antennas and by incomplete Channel State Information(CSI).

1.1.1 Open-Loop Spatial Multiplexing

In case of open-loop spatial multiplexing, the transmitter operates with no information about the channel state. In open loop systems, the channel information may or may not be available at the receiver. If the channel information is not available then open loop systems are in general affected by high channel correlation. However, if the channel information is present at the receiver then the antenna correlation may be removed. The most straight forward method would be a direct channel inversion, but for reasons discussed later this does not yield desirable results and is usually avoided. Some open loop systems such as the QR decomposition based methods can be robust (Wolniansky *et al.* (1998)).

1.1.2 Closed-Loop Spatial Multiplexing

Closed-loop spatial multiplexing mode allows for feedback from the receiver to the transmitter. Thus, the transmitter may have complete or partial knowledge of the channel state. The channel state information can be used to overcome the channel correlation and help in achieving simpler receiver architectures. The prefered closed loop system is a linear TRx based on the SVD of the channel matrix (Goldsmith (2005), also discussed in Chapter 2). Though there has been a lot of recent research on maximizing the utility of MIMO (Mietzner *et al.* (2009)), there is still scope for improvement in practical MIMO systems.

1.2 Motivation

An interesting transceiver design based on a matrix decomposition known as Generalised Triangular Decomposition, was introduced by Jiang *et al.* (2008). The GTD family of transceivers were shown to be optimal by Weng *et al.* (2010). This project was started in an attempt to extend the results on GTD TRxs to scenarios accounting for some practical constraints. In this report, we shall be looking at closed loop spatial multiplexing scenarios with limited feedback, performance when channel estimation error is accounted for and try to obtain a bit allocation formula for the limited feedback.

In the course of the project, various interesting observations were made and these have led to the analysis of precoder matrices and we have obtained some insights into conditioning of noise by precoders. This thesis studies the optimal Grassman subspace packing introduced by Love and Heath (2005) and we arrived at a low complexity codebook size reduction algorithm which has provided some novel observations.

1.3 Organization of Thesis

This thesis is organized as follows - in Chapter 2, the common closed-loop spatial multiplexing systems are reviewed. These systems are studied by means of matlab simulations and analysis of BER vs SNR plots, which are presented in Chapter 3. Limited feedback systems are reviewed in Chapter 4. In Chapter 5, simulations and analysis of limited feedback systems are provided. Also, a sub-optimal precoder codebook reduction algorithm is discussed and some interesting simulation results are analysed in Chapter 5. Chapter 6 includes the study of masking the channel estimation errors by the quantization noise. Finally, Chapter 7 holds the conclusion and possible problems for future study.

CHAPTER 2

Closed Loop MIMO Systems

As discussed in 1.1.2, closed-loop systems allow for feedback from the receiver to the transmitter. The type of feedback may vary depending the design of the transceiver. Some commonly used MIMO transceiver designs make use of matrix decompositions such as SVD, GMD or QR (SVD is the most prevalent), of these SVD and GMD type transceivers require the transmitter to know the precoder matrix which has to be fedback from the receiver. In addition to the precoder information, the optimal rate of transmission/ bit allocation is also fedback. In LTE, this is referred to as the Channel Quality information (CQI). The following sections will review some common closed loop MIMO transceiver designs. For illustration purpose let us adopt the following system model.

2.1 System Model

Suppose the transmitted symbol vector is represented by $\mathbf{s}$ and the channel matrix is $\mathbf{H}$, where $\mathbf{H}$ is a $N_r \times N_t$ complex matrix, $\mathbf{s}$ is $N_t \times 1$ vector, then the recieved vector $\mathbf{y}$ is given by

$$\mathbf{y} = \mathbf{Hs} + \mathbf{n}$$

where $\mathbf{n}$ is the noise vector. We shall assume that the noise vector consists of i.i.d random variables and each being AWGN.

2.2 Singular Value Decomposition (SVD) in MIMO

The channel matrix $\mathbf{H}$, can be decomposed using SVD as follows,

$$\mathbf{H} = \mathbf{QRP^H}$$

where $\mathbf{Q}$ and $\mathbf{P}$ are unitary matrices, while $\mathbf{R}$ is the singular value matrix, which is diagonal with $R_{ii} = \sigma_i$, $i = 1, 2, ..N$. where σ_i represent the singular values of $\mathbf{H}$ and $N = min(N_r, N_t)$.

Since the transmitter has perfect channel state information, the matrix $\mathbf{P}$ is used as the precoder matrix on the symbol vector($\mathbf{s}$) before transmission and a gain matrix, $\mathbf{R^{-1}Q^H}$, is used on the receiver side. Then the received symbol vector($\mathbf{y}$) would be given by

$$\begin{aligned} \mathbf{y} &= \mathbf{R^{-1}Q^HHPs} + \mathbf{R^{-1}Q^Hn} \\ &= \mathbf{R^{-1}Rs} + \mathbf{R^{-1}Q^Hn} \\ &= \mathbf{s} + \mathbf{R^{-1}Q^Hn} \end{aligned}$$

since, $\mathbf{Q^H}$ is a unitary matrix, $\mathbf{Q^Hn}$ is still a vector of zero mean normal random variables with covariance $\mathbf{QC_nQ^H}$, where the covariance of $\mathbf{n}$ is $\mathbf{C_n} = \sigma_n^2\mathbf{I}$, σ_n being a scalar. Thus, the covariance of the transformed noise ($\mathbf{Q^Hn}$) is given by,

$$\mathbf{QC_nQ^H} = \sigma_n^2\mathbf{QIQ^H} = \sigma_n^2\mathbf{I}$$

Therefore, each stream may now be treated independently as N streams in parallel each with SNR scaled by $\frac{1}{[R_{ii}]^2}$. Since the SVD transceiver design involves only linear transformations, it is a linear transceiver.

Figure 2.1: Block Diagram of SVD based MIMO Transceiver

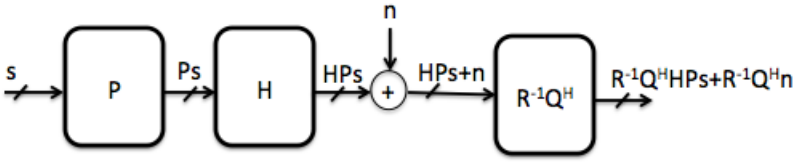

2.3 QR Decomposition

Another commonly known decomposition is the QR decomposition, according to which a square matrix $\mathbf{A}$ maybe decomposed as

$$\mathbf{A} = \mathbf{QR}$$

where, $\mathbf{Q}$ is unitiary while $\mathbf{R}$ is upper triangular. However, if A is rectangular $m \times n$, with $m \geq n$, then it can be decomposed into a product of a $m \times m$ unitary matrix $\mathbf{Q}$, and $m \times n$ upper triangular matrix $\mathbf{R}$.

A QR type MIMO transceiver uses an identity precoder matrix and multiplies the received vector by a gain matrix $(diag([\mathbf{R}_{N\times N}])^{-1}\mathbf{Q^H}$, the vector($\mathbf{y}$) at the demodulator is given by,

$$\begin{aligned} \mathbf{y} &= (diag([\mathbf{R_{N\times N}}])^{-1}\mathbf{Q^H Hs} + (diag([\mathbf{R_{N\times N}}])^{-1}\mathbf{Q^H n} \\ &= (diag([\mathbf{R_{N\times N}}])^{-1}\mathbf{Rs} + (diag([\mathbf{R_{N\times N}}])^{-1}\mathbf{Q^H n} \end{aligned}$$

where $(diag([\mathbf{R}_{N\times N}])^{-1}\mathbf{R}$ is upper triangular with the diagonal elements equal to unity. If a feedback matrix $\mathbf{B}$ is chosen such that $(diag([\mathbf{R}_{N\times N}])^{-1}\mathbf{R}\text{-}\mathbf{B} = \mathbf{I}$, then processed vector after the feedback step is given as

$$\hat{\mathbf{y}} = \mathbf{y} - \mathbf{B}\hat{\mathbf{s}}$$

where $\hat{\mathbf{s}}$ is decision output from the demodulator. Under high SNR values it is fair to assume that $\hat{\mathbf{s}} = \mathbf{s}$. Thus,

$$\hat{\mathbf{y}} = \mathbf{s} + (diag([\mathbf{R_{N\times N}}])^{-1}\mathbf{Q^H n}$$

Figure 2.2: Block Diagram of QR based MIMO Transceiver

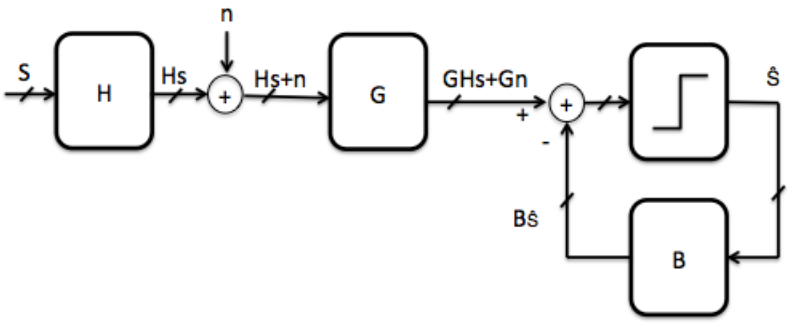

2.4 Generalized Triangular Decomposition (GTD)

Multiplicative Majorization: Given vectors $[\mathbf{a}_1, \mathbf{a}_2, ..\mathbf{a}_n]$ and $[\mathbf{b_1}, \mathbf{b}_2, ..\mathbf{b}_n]$ with $\mathbf{a}_i$ and $\mathbf{b}_i$ being positive for $i = 1, ..n$. Then $\mathbf{a}$ is said to be multiplicatively majorized by $\mathbf{b}$, $\mathbf{a} \prec_\times \mathbf{b}$, if

$$\prod_{i=1}^{n} \mathbf{a}_{[i]} \leq \prod_{i=1}^{n} \mathbf{b}_{[i]}$$

where $[i]$ denotes the element of the vector with the i-th biggest component.

If $\mathbf{H}$ is a rank K, $m \times n$ matrix, with singular values $\sigma_1, \sigma_2.., \sigma_K$ and let $\mathbf{r}$ be a vector satisfying,

$$\mathbf{a} \prec_\times \mathbf{h}$$

where $\mathbf{a} = [|\mathbf{r}_1|, |\mathbf{r}_2|, .., |\mathbf{r}_K|]$ and $h = [\sigma_1, \sigma_2, .., \sigma_K]$. Then there exist $\mathbf{R}$, $\mathbf{P}$ and $\mathbf{Q}$ such that

$$\mathbf{H} = \mathbf{QRP^H}$$

where $\mathbf{Q}, \mathbf{P}$ are unitary while $\mathbf{R}$ is an upper triangular matrix (Weng *et al.* (2010)). This decomposition is referred to as GTD since decompositions such as SVD, GMD, QR etc. are specific cases of GTD.

Figure 2.3: Block Diagram of GTD based MIMO Transceiver

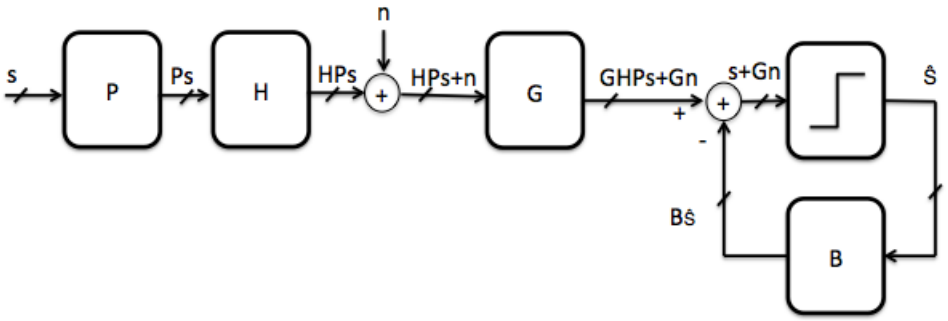

2.5 GTD-based MIMO system

A transceiver design based on GTD was proposed in Jiang *et al.* (2008). The structure is similar to the QR DFE type transceiver, however, the GTD transciever uses a precoder matrix on the transmitter side. The advantage of a unitary precoder transformation was explained in the section-2.2, this holds for GTD (hence in QR and GMD) as well.

Suppose the channel matrix can be decomposed as per the Generalised Triangular Decomposition explained above. Then the antenna correlation can be eliminated by using a DFE type transceiver. The transceiver would use precoder matrix $\mathbf{P}$, a gain matrix $\mathbf{G} = (diag([\mathbf{R_{N\times N}}])^{-1})\mathbf{Q^H}$ on the receiver side and feedback matrix $\mathbf{B}(= \mathbf{GHP} - \mathbf{I})$. The vector $\mathbf{y}$ prior to the feedback step and $\hat{\mathbf{y}}$ after the feedback step would be as follows,

$$\begin{aligned} \mathbf{y} &= (diag([\mathbf{R_{N\times N}}])^{-1}\mathbf{Q^H HPs} + (diag([\mathbf{R_{N\times N}}])^{-1}\mathbf{Q^H n} \\ &= (diag([\mathbf{R_{N\times N}}])^{-1}\mathbf{Rs} + (diag([\mathbf{R_{N\times N}}])^{-1}\mathbf{Q^H n} \end{aligned}$$

$$\hat{\mathbf{y}} = \mathbf{y} - \mathbf{B}\hat{\mathbf{s}}$$

where $\hat{\mathbf{s}}$ is decision, under high SNR values it is fair to assume that $\hat{\mathbf{s}} = \mathbf{s}$. Thus,

$$\hat{\mathbf{y}} = \mathbf{s} + (diag([\mathbf{R_{N\times N}}])^{-1}\mathbf{Q^H n}$$

QR, GMD and SVD are specific cases of GTD. In $\mathbf{H} = \mathbf{QRP^H}$, if P is set to $\mathbf{I}$, then we obtain QR decomposition, if $\mathbf{R}$ is constrained to be diagonal then it will result in SVD, and if the diagonal elements of $\mathbf{R}$ are constrained to be equal then we have GMD.

The advantage with GMD is that there is no need for bit allocation or power allocation as each channel is equivalent. Jiang *et al.* (2005a) introduced the GMD based MIMO transceiver, it is similar to the GTD based transceiver. Though GMD is simpler than GTD, Jiang *et al.* (2005b) showed that GMD based TRx can achieve near capacity performance.

2.6 Bit Allocation

The other information that is usually fedback is the number of bits to be allocated to each stream. It is intuitive that to improve performance, greater number of bits should be transmitted across a channel with high SNR compared to a channel with low SNR. The concept of bit allocation is based on the above principle. It has been shown that the optimal bit loading formula for a linear transceiver that achieves minimum transmit power while ensuring a certain performance criteria (Lin and Phoong (2001)) is given by

$$b_k = D - \log_2 c_k + \log_2(\sigma_k^2)$$

where, b_k is the number of bits to be loaded onto the k^{th} stream, σ_k is the k^{th} singular value of the channel matrix ($\mathbf{H}$), $c_k = \frac{\sigma_n^2}{3}(Q^{-1}(\frac{P_e(k)}{4}))^2$ and $P_e(k)$ is the max. probability of error allowed on the k^{th} stream. D is a scalar constant chosen such that $\sum_{k=1}^{n} b_k = b$, where b is a constant representing the total number of bits that is to be allocated between the n streams. A similar result for the GTD transceiver has been derived in Weng *et al.* (2010) and is given by

$$b_k = D - \log_2 c_k + \log_2([\mathbf{R}_{kk}]^2)$$

The b_k value is obtained without any integer constraint, however, since GTD is not an unique decomposition, R_{kk} in the GTD case can be chosen in such a way that b_k is an integer. Hence, the performance of the GTD transceiver is expected to be marginally better than the linear transceivers. Weng *et al.* (2010) also showed that the GTD family of transceivers lead to optimal BER performance under power constraints.

Interestingly, the power $(P_1, ..P_N)$ allocated to each of the streams in the optimal

transceiver is equal and given by,

$$P_k = 2^D$$

This is significant because equal power allocation is desired for the power amplifiers at the transmitter.

CHAPTER 3

Performance Evaluation - Ideal Feedback

For the purpose of analysis it is common to assume complete CSIT or ideal feedback. In the following simulations, perfect feedback is assumed. The BER vs SNR curves are presented along with the analysis and inferences drawn from them.

3.1 Simulation setting and assumptions

We assume a 4×4 channel (4 transmitting and 4 receiving antennas), with each element of the channel matrix following rayleigh statistics (complex gaussian). Also, the simulations are performed under assumption of complete CSIT. The symbol vector comprises of symbols from square QAMs if the number of bits is even or else rectangular QAMs are used. If the number of bits allocated to the k^{th} stream ($\hat{b_k}$) is $2n+1$, then the symbol is chosen from a $2^n \times 2^{(n+1)}$ QAM. For the sake of simplicity the noise is taken to be complex gaussian with unit variance ($\mathcal{N}(0,1)$), we assume that the channel does not cause any dispersion, thus, the pulse shaping step is skipped as it will not lead to any change in the simulation result. The number of bits ($\hat{b_k}$) allocated to each stream is obtained by rounding the value obtained from the bit allocation formula (b_k) , thus, on average $\sum_{k=1}^{n} \hat{b_k} = \sum_{k=1}^{n} b_k$, hence, this would be a fair comparison between GTD and the other transceiver designs. The total number of bits $b = \sum_{k=1}^{n} b_k$ is constrained and the total power used for transmission is also constrained. Each block has 10 sets of symbol vectors to be transmitted and the BER is averaged over 1000 such blocks. Since the noise is Gaussian, a shortest euclidean distance decoder is used to decode each stream at the receiver.

Figure 3.1: BER vs SNR, Comparison between ideal SVD, QR, GTD and GMD. Each stream consists of symbols from 16-QAM (no bit allocation)

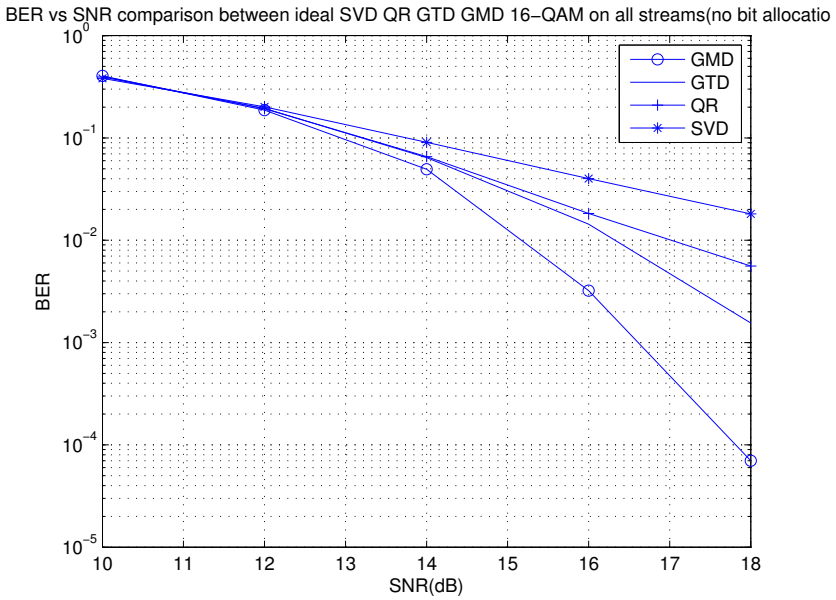

Going back to the bit allocation formula in section 2.6, we see that for the same maximum allowed probability of error ($P_e(k)$) for each stream (meaning $c_k = const$) the bits (b_k) allocated to each stream is a function of the corresponding diagonal element ($\mathbf{R_{kk}}$). Given that GMD leads to equal diagonal elements in $\mathbf{R}$, equal bit allocation represents the optimal scheme for the GMD-TRx. Hence, with equal bits allocated to each stream, we expect GMD to outperform the rest of the methods as verified in figure(3.1). Interestingly, with equal bit allocation, QR is performing better than SVD. Thus, bit-loading is somehow having a higher impact on SVD than on QR.

As seen in figure(3.2), the schemes perform close to the optimal GTD scheme when the bit allocation formula is used, though QR and SVD based TRx are expected to be slightly sub-optimal due to the rounding of the bits to be allocated.

We obtain similar results (Figure 3.3 and Figure 3.4) when fewer bits (8 bits) transmitted. However, it is observed that the relative degradation with equal bit allocation is much higher when fewer bits are used.

Figure 3.2: BER vs SNR, Comparison between ideal SVD, QR, GTD and GMD. Bits were allocated to each stream using the optimal bit allocation formula

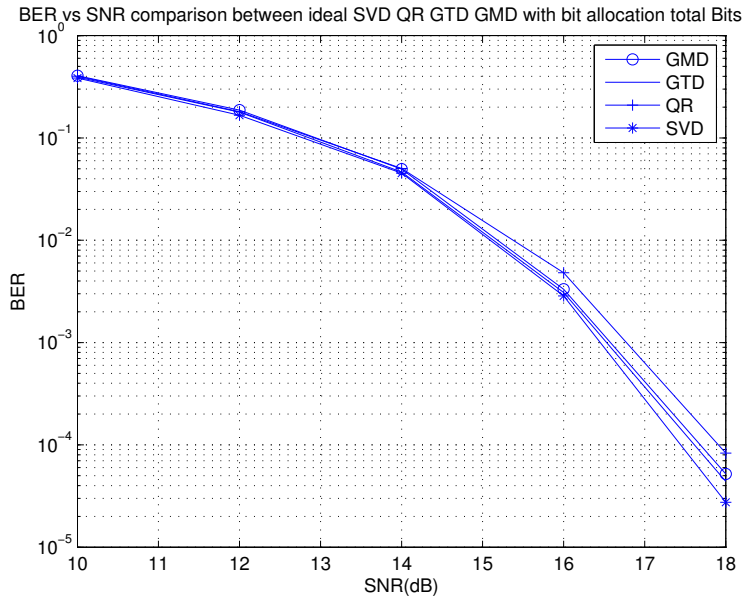

Figure 3.3: BER vs SNR, Comparison between ideal SVD, QR, GTD and GMD, with equal number of bits allocated for each stream (QPSK on all streams,$b = 8$)

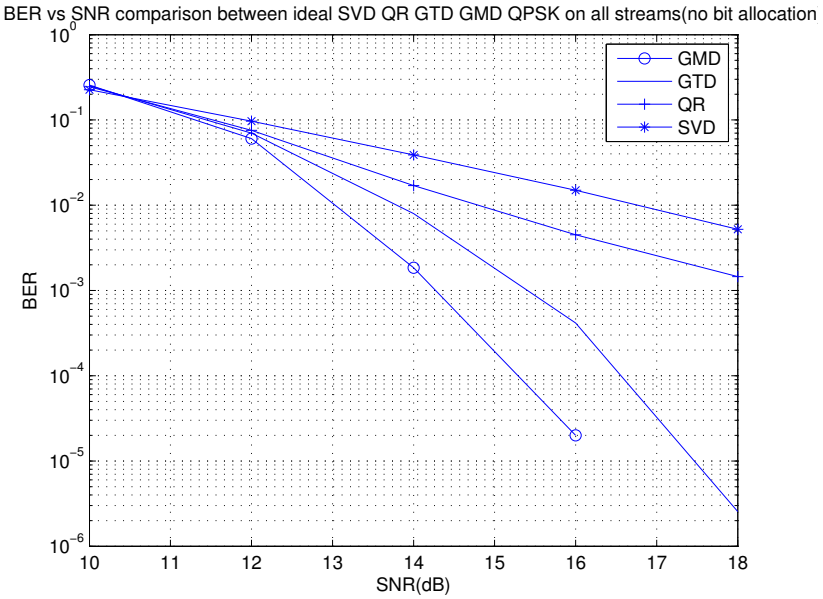

Figure 3.4: BER vs SNR,Comparison between ideal SVD, QR, GTD and GMD, $b = 8$ Bits allocated using the optimal bit allocation formula

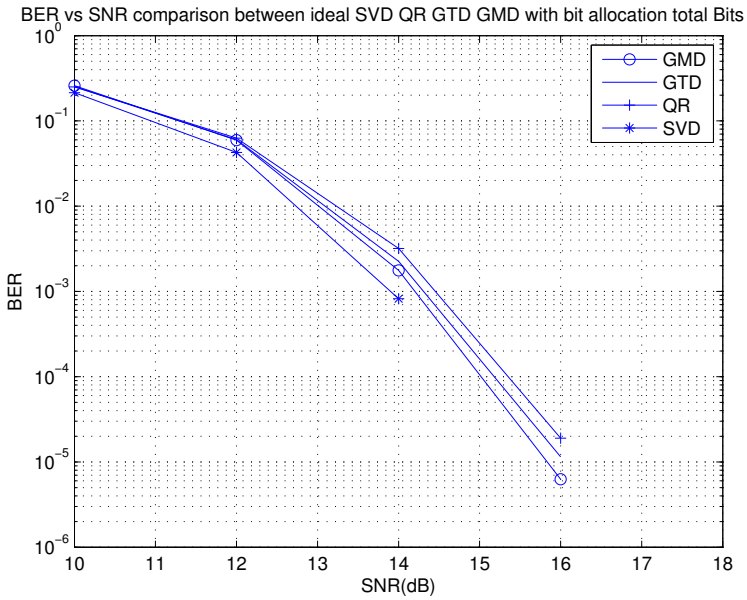

3.1.1 Effect of estimation error on BER

Perfect channel estimation was assumed in the previous simulations, however, it is impossible to achieve such a perfect channel estimate. Thus, inorder to measure the performance of these MIMO Trx designs under more practical conditions, we need to account for channel estimation errors ($\triangle\mathbf{H}$). Thus, if the channel estimate is given by $\mathbf{H}$ then the actual channel would have been $\mathbf{H} + \triangle\mathbf{H}$.

The conventional method to account for channel estimation errors is perturbation of the channel coefficients by addition of noise. In the following simulation, estimation error was introduced by addition of a random matrix ($-\triangle\mathbf{H} = \mathbf{h}$) to $\mathbf{H}$, with each element of $\mathbf{h}$ from $\mathcal{N}(0, 0.1)$.

It is obvious that the channel estimation errors will lead to poorer performance of the MIMO and the following results verify the same.

Figure 3.5: BER vs SNR, Comparison between ideal SVD, QR, GTD and GMD in the presence of channel estimation errors (h_{ij} from $\mathcal{N}(0, 0.1)$) with equal number of bits allocated on each stream (16-QAM on all streams, $b = 16$)

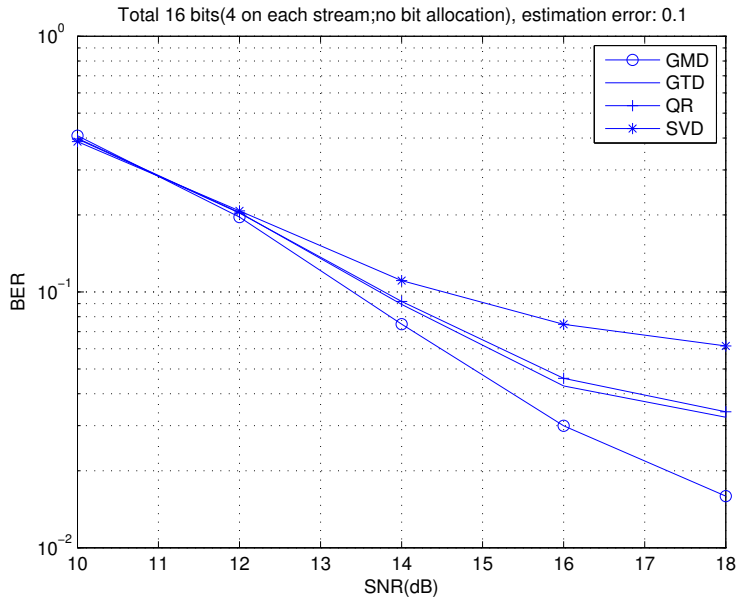

Figure 3.6: BER vs SNR, Comparison between ideal SVD, QR, GTD and GMD in the presence of channel estimation errors (h_{ij} from $\mathcal{N}(0, 0.1)$) with $b = 16$ bits allocated using the optimal bit allocation formula

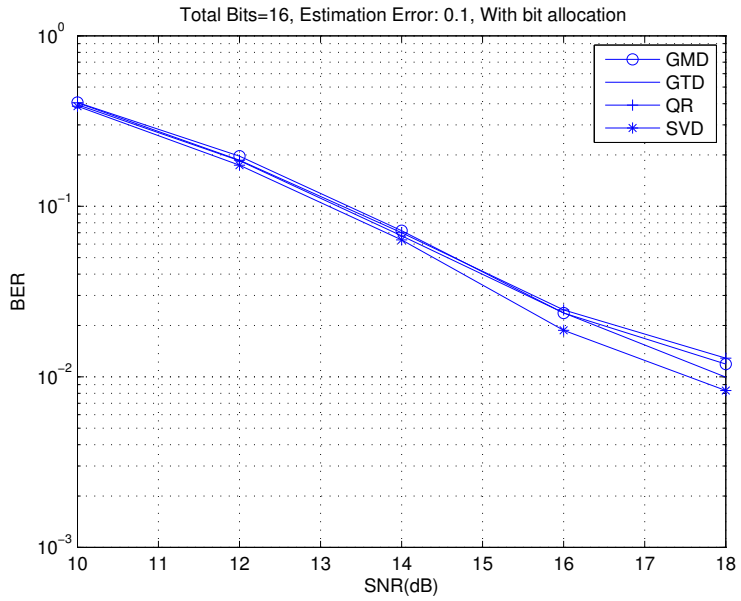

It is observed from Fig-3.5 and Fig-3.6 that even with a small perturbation ($\mathcal{N}(0, 0.1)$), the advantage in bit allocation is lost to a large extent. In this particular case the QR receiver achieves 10^{-2} compared to $10^{-1.8}$ at 18dB SNR. Thus, there is lesser incentive to compute the bit allocation scheme if the channel estimation is not accurate.

CHAPTER 4

Limited Feedback Systems

If perfect channel information is known at the transmitter, then the methods discussed in Chapter 2 can be used for designing the transceiver. However, this would not be feasible in practical applications as only a few bits can be fedback. In these scenarios, a predetermined codebook is used. A codebook is a finite collection of precoder matrices. The receiver sends the precoder index and the transmitter chooses the corresponding precoder matrix from the finite set. Now there are 2 questions, how is the codebook designed and how does the receiver decide the precoder matrix.

4.1 Codebook Design Criteria and Precoder selection

4.1.1 Grassman Subspace Packing

If $U(M_t, M)$ represents the set of all $M_t \times M$ matrices with orthonormal columns, then each matrix in $U(M_t, M)$ represents an M-dimensional subspace of $\mathcal{C}^{\mathrm{M}}$. The set of subspaces spanned by all the matrices in $U(M_t, M)$ is refered to as the grassman manifold $\mathcal{G}(M_t, M)$. Finding $N(\geq 1)$ matrices in $U(M_t, M)$ that maximize the minimum subspace distance is called as *Grassmanian subspace packing.* The distance measures commonly used for distance between subspaces are 1. Chordal Distance, 2. Fubini-Study distance and 3.Projection 2-norm

$$d_{chord}(\mathbf{F_1}, \mathbf{F_2}) = \frac{1}{\sqrt{2}}||\mathbf{F_1}\mathbf{F_1^*} - \mathbf{F_2}\mathbf{F_2^*}||_F = \sqrt{M - \sum_{i=1}^{M} \lambda_i^2\{\mathbf{F_1^*}\mathbf{F_2}\}}$$

$$d_{FS}(\mathbf{F_1}, \mathbf{F_2}) = \arccos|\det(\mathbf{F_1^*}\mathbf{F_2})|$$

$$d_{proj}(\mathbf{F_1}, \mathbf{F_2}) = ||\mathbf{F_1}\mathbf{F_1^*} - \mathbf{F_2}\mathbf{F_2^*}||_2 = \sqrt{1 - \lambda_{min}^2\{\mathbf{F_1^*}\mathbf{F_2}\}}$$

Love and Heath (2005) showed that depending on the selection criteria the grassman packing with a certain distance measure leads to the optimal codebook design. Since, we require the minimization of BER, we shall use the projection 2-norm as precribed by Love and Heath (2005).

4.1.2 MIMO in LTE

In LTE, feedback for the MIMO transmitter include Channel Quality Information (CQI), Precoder Matrix information (PMI) and Rank Index (RI). The feedback might be wide-band CSI or frequency selective. RI is a single value of 2 bits for a 4 antenna system and 1 bit for a 2 antenna system. It represents the rank of the channel matrix, which is also the number of streams that can be efficiently transmitted with spatial multiplexing. PMI is computed by the receiver and is a number that maps to a precoder in the LTE codebook. The calculation of PMI value (0 to 3 for 2 antenna systems and 0 to 15 for 4 antenna systems) is conditioned on the RI value. CQI takes 16 values which represent a combination of modulation alphabets and code rates. Since CQI is indicative of the maximum rate of transmission that will satisfy BLER$\leq$10%, it represents the effective SNR of the system, hence it is obtained by mapping a vector of SNR values (corresponding to the multiple streams) to a single SNR value. The common mapping schemes are EESM and MIESM (Schwarz *et al.* (2010)). The computation of these feedback bits might follow algorithms similar to the one below (Frenger-EricsonResearch (2009)).

Algorithm 1 CSI COMPUTATION IN LTE

1. for each RI do
   (a) for each PMI do
      i. compute SINR per layer
      ii. SINRs -> predicted throughput
2. Select RI,PMI combination that leads to maximum throughput
3. Given the selected RI and PMI
   (a) Find the CQI (the modulation scheme and coding) that leads to a BLER $\leq$ 10% with highest data rate.

LTE Codebook

LTE supports transmission of 2 or 4 codewords at a time. However, depending on the channel rank LTE supports 1 to 4 layers.

Table 4.1: 4 Tx LTE precoder codebook

Code--book Index	$\mathbf{u_i}$	1	2	3	4
0	$[1\ -1\ -1\ -1]^T$	$\mathbf{W}_0^{\{1\}}$	$\mathbf{W}_0^{\{14\}}/\sqrt{2}$	$\mathbf{W}_0^{\{124\}}/\sqrt{3}$	$\mathbf{W}_0^{\{1234\}}/2$
1	$[1\ -j\ -1\ j]^T$	$\mathbf{W}_1^{\{1\}}$	$\mathbf{W}_1^{\{12\}}/\sqrt{2}$	$\mathbf{W}_1^{\{123\}}/\sqrt{3}$	$\mathbf{W}_1^{\{1234\}}/2$
2	$[1\ 1\ -1\ 1]^T$	$\mathbf{W}_2^{\{1\}}$	$\mathbf{W}_2^{\{12\}}/\sqrt{2}$	$\mathbf{W}_2^{\{123\}}/\sqrt{3}$	$\mathbf{W}_2^{\{3214\}}/2$
3	$[1\ j\ 1\ -j]^T$	$\mathbf{W}_3^{\{1\}}$	$\mathbf{W}_3^{\{12\}}/\sqrt{2}$	$\mathbf{W}_3^{\{123\}}/\sqrt{3}$	$\mathbf{W}_3^{\{3214\}}/2$
4	$[1\ (-1-j)/\sqrt{2}\ -j\ (1-j)/\sqrt{2}]^T$	$\mathbf{W}_4^{\{1\}}$	$\mathbf{W}_4^{\{14\}}/\sqrt{2}$	$\mathbf{W}_4^{\{124\}}/\sqrt{3}$	$\mathbf{W}_4^{\{1234\}}/2$
5	$[1\ (1-j)/\sqrt{2}\ -j\ (-1-j)/\sqrt{2}]^T$	$\mathbf{W}_5^{\{1\}}$	$\mathbf{W}_5^{\{14\}}/\sqrt{2}$	$\mathbf{W}_5^{\{134\}}/\sqrt{3}$	$\mathbf{W}_5^{\{1234\}}/2$
6	$[1\ (1+j)/\sqrt{2}\ -j\ (-1+j)/\sqrt{2}]^T$	$\mathbf{W}_6^{\{1\}}$	$\mathbf{W}_6^{\{13\}}/\sqrt{2}$	$\mathbf{W}_6^{\{134\}}/\sqrt{3}$	$\mathbf{W}_6^{\{1324\}}/2$
7	$[1\ (-1+j)/\sqrt{2}\ -j\ (1+j)/\sqrt{2}]^T$	$\mathbf{W}_7^{\{1\}}$	$\mathbf{W}_7^{\{13\}}/\sqrt{2}$	$\mathbf{W}_7^{\{124\}}/\sqrt{3}$	$\mathbf{W}_7^{\{1324\}}/2$
8	$[1\ -1\ 1\ 1]^T$	$\mathbf{W}_8^{\{1\}}$	$\mathbf{W}_8^{\{12\}}/\sqrt{2}$	$\mathbf{W}_8^{\{124\}}/\sqrt{3}$	$\mathbf{W}_8^{\{1234\}}/2$
9	$[1\ -j\ -1\ -1j]$	$\mathbf{W}_9^{\{1\}}$	$\mathbf{W}_9^{\{14\}}/\sqrt{2}$	$\mathbf{W}_9^{\{134\}}/\sqrt{3}$	$\mathbf{W}_9^{\{1234\}}/2$
10	$[1\ 1\ 1\ -1]^T$	$\mathbf{W}_{10}^{\{1\}}$	$\mathbf{W}_{10}^{\{13\}}/\sqrt{2}$	$\mathbf{W}_{10}^{\{123\}}/\sqrt{3}$	$\mathbf{W}_{10}^{\{1324\}}/2$
11	$[1\ j\ -1\ j]$	$\mathbf{W}_{11}^{\{1\}}$	$\mathbf{W}_{11}^{\{13\}}/\sqrt{2}$	$\mathbf{W}_{11}^{\{134\}}/\sqrt{3}$	$\mathbf{W}_{11}^{\{1324\}}/2$
12	$[1\ -1\ -1\ 1]^T$	$\mathbf{W}_{12}^{\{1\}}$	$\mathbf{W}_{12}^{\{12\}}/\sqrt{2}$	$\mathbf{W}_{12}^{\{123\}}/\sqrt{3}$	$\mathbf{W}_{12}^{\{1234\}}/2$
13	$[1\ -1\ 1\ -1]^T$	$\mathbf{W}_{13}^{\{1\}}$	$\mathbf{W}_{13}^{\{13\}}/\sqrt{2}$	$\mathbf{W}_{13}^{\{123\}}/\sqrt{3}$	$\mathbf{W}_{13}^{\{1324\}}/2$
14	$[1\ 1\ -1\ -1]^T$	$\mathbf{W}_{14}^{\{1\}}$	$\mathbf{W}_{14}^{\{13\}}/\sqrt{2}$	$\mathbf{W}_{14}^{\{123\}}/\sqrt{3}$	$\mathbf{W}_{14}^{\{3214\}}/2$
15	$[1\ 1\ 1\ 1]^T$	$\mathbf{W}_{15}^{\{1\}}$	$\mathbf{W}_{15}^{\{12\}}/\sqrt{2}$	$\mathbf{W}_{15}^{\{123\}}/\sqrt{3}$	$\mathbf{W}_{15}^{\{1234\}}/2$

Where $W_i^{\{c_1,c_2..c_m\}}$ is the matrix defined by the columns $c_1, c_2..c_m$ of matrix W_i , where W_i is the house holder transform on u_i , $\mathbf{W_i} = \mathbf{I_{4\times 4}} - 2\mathbf{u_i}\mathbf{u_i^H}/\mathbf{u_i^H}\mathbf{u_i}$.

Table 4.2: 2 Tx Precoder Codebook

Codebook index	1 layer	2 layer
0	$\frac{1}{\sqrt{2}}\begin{bmatrix}1\\1\end{bmatrix}$	-
1	$\frac{1}{\sqrt{2}}\begin{bmatrix}1\\-1\end{bmatrix}$	$\frac{1}{2}\begin{bmatrix}1 & 1\\1 & -1\end{bmatrix}$
2	$\frac{1}{\sqrt{2}}\begin{bmatrix}1\\j\end{bmatrix}$	$\frac{1}{2}\begin{bmatrix}1 & 1\\j & -j\end{bmatrix}$
3	$\frac{1}{\sqrt{2}}\begin{bmatrix}1\\-j\end{bmatrix}$	-

4.2 Selection of Precoder

Given a codebook, we may choose the precoder based on the following selection criteria: 1.precoder that minimizes the theoretical probability of error, 2.precoder that maximizes the mutual information or 3. Simply quantize the ideal precoder matrix to the closest one in the codebook, for which a matrix norm has to be adopted.

With ideal feedback (Love and Heath (2005)) shows that the SVD precoder is optimal under selection criteria 1 and 2.

CHAPTER 5

Performance Evaluation - Limited Feedback

Figure 5.1: BER vs SNR, Comparison between Limited feedback (Grassman codebook with 256 precoders) SVD and ideal SVD based MIMO TRx, using a 5x4 MIMO system with only QPSK symbols on each stream

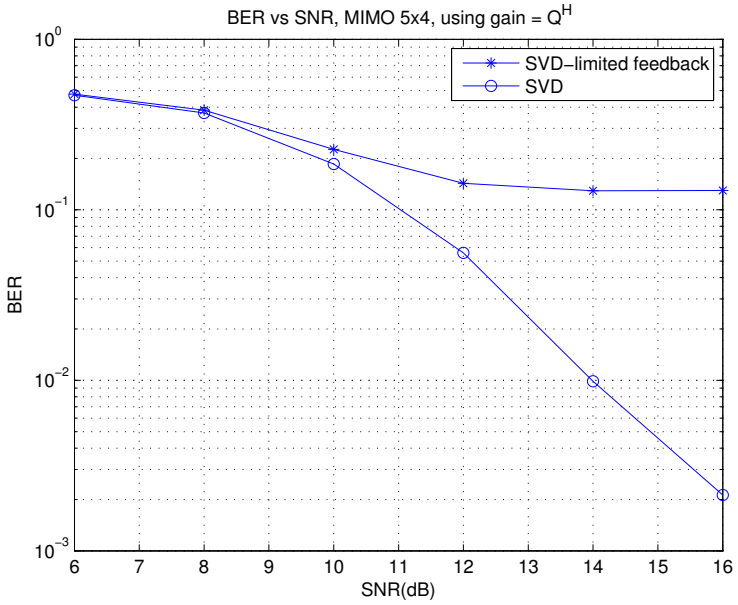

The grassman codebook used for the following simulations were obtained from (Grassman Tables by D.Love). If we view the limited feedback SVD merely as quantization of the optimal precoder and implement the receiver design as in case of the perfect feedback, we observe very poor results. The quantization noise is very high as the BER values floor at a low $\frac{E_b}{N_0}$ value.

If we take the quantized precoder to be $\mathbf{P} + \mathbf{\Delta P}$ then the received symbol vector is

$$\begin{aligned} y &= \mathbf{R^{-1}Q^H H}(\mathbf{P} + \mathbf{\Delta P})s + \mathbf{Q^H}n \\ &= \mathbf{R^{-1}Q^H QRP^H}(\mathbf{P} + \mathbf{\Delta P})s + \mathbf{Q^H}n \\ &= \mathbf{P^H P}s + \mathbf{P^H \Delta P}s + \mathbf{Q^H}n \\ &= s + \mathbf{P^H \Delta P}s + \mathbf{R^{-1}Q^H}n \end{aligned}$$

The quantization noise ($\mathbf{P^H \Delta P} s$), which in this particular case is causing the BER curve to floor at 12dB, increases as the signal strength increases.

5.1 Modified Linear Receiver - Channel Inversion

Instead of using the receiver gain of $\mathbf{R^{-1}Q^H}$ as in the perfect feedback case, we now try to perform a channel inversion, i.e. use $(\mathbf{HP})^{-1}$.

$$\begin{aligned} \mathbf{G} &= (\mathbf{HP'})^{-1} \\ &= (\mathbf{QRP^H P'}) - 1 \end{aligned}$$

$$\begin{aligned} y &= \mathbf{GHP'}s + \mathbf{G}n \\ &= s + (\mathbf{HP'})^{-1}n \end{aligned}$$

Figure 5.2: BER vs SNR, Comparison between ideal SVD and modified limited feedback linear TRx (Grassman codebook with 256 precoders) using a 5×4 MIMO system with only QPSK symbols on each stream

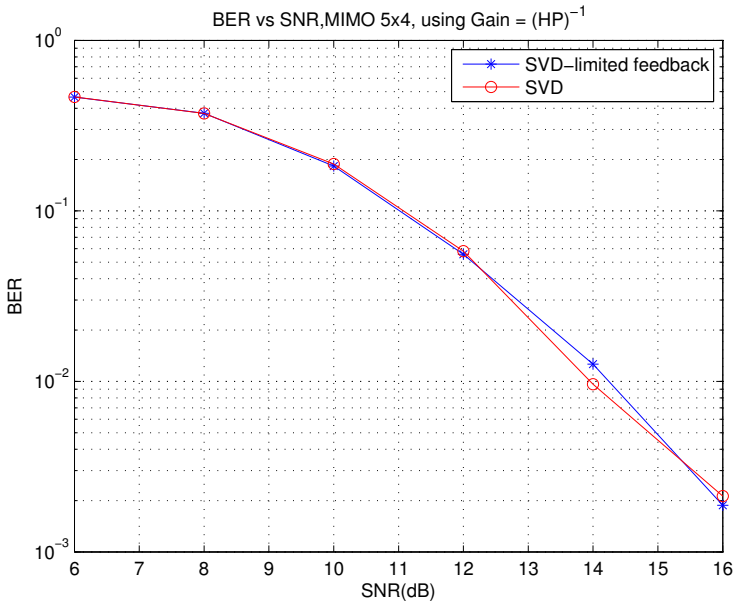

Here the channel inversion may lead to noise enhancement and noise charachteristics are completely changed. However, the quantization noise that was degrading the performance is no longer present. Most importantly this system is almost able to match

the SVD TRx with ideal feedback. In Chapter 2, it was mentioned that the advantage of SVD was in the unitary transformation, thus, unless there is an advantage that the precoder provides, the modified method is similar to direct channel inversion.

Figure 5.3: BER vs SNR, Comparison between Direct Channel Inversion and Inversion after the use of Precoder

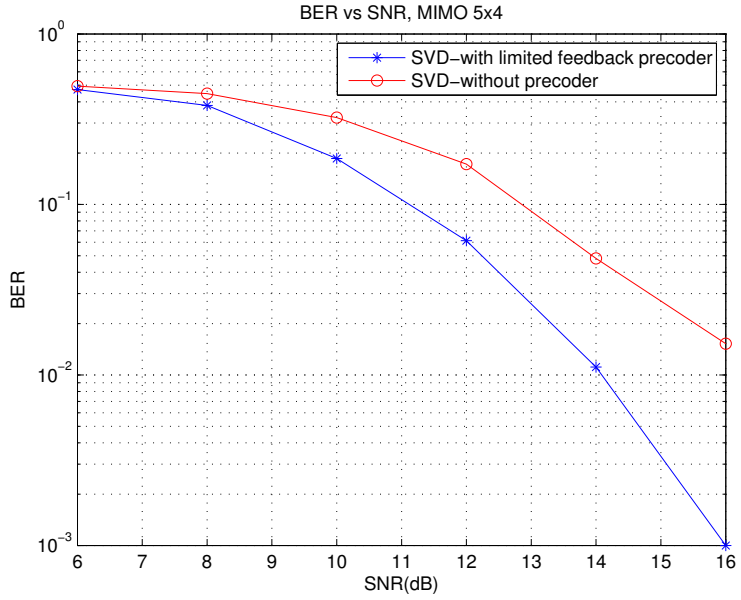

From the plot it can be seen that the precoder is effective as it leads to a much better performance, though the receiver is inverting the channel in both cases. When the precoder is an identity matrix or when no precoder is used, the received vector would be given by

$$y = s + \mathbf{H^{-1}}n$$

as against

$$y = s + (\mathbf{P}')^{\mathbf{H}}\mathbf{H^{-1}}n$$

with the use of a precoder.

The effective SNR value remains the same in both cases, however, the precoder is causing some conditioning of noise.

5.2 Why does inversion work?

The received symbol vector after channel inversion would be the following.

$$\mathbf{y} = \mathbf{s} + \mathbf{H}^{-1}\mathbf{n} \tag{5.1}$$

$$\mathbf{y} = \mathbf{s} + \mathbf{P}^{\mathbf{H}}\mathbf{H}^{-1}\mathbf{n} \tag{5.2}$$

(1) represents the case with no precoder and (2) is with the precoder.

Since the demodulation algorithm at the receiver is treating each stream independently, the noise variance determines the BER of the corresponding stream. In the following simulations, the noise vector($\mathbf{n}$) is treated as 4 distinct noise random variables. The following plot represents the frequency of occurrence of the noise samples, which in turn is a scaled version of the marginal pdf itself.

Figure 5.4: Impact of (limited feedback) precoder on Noise. Plot of frequency of occurence of noise samples(scaled pdf)

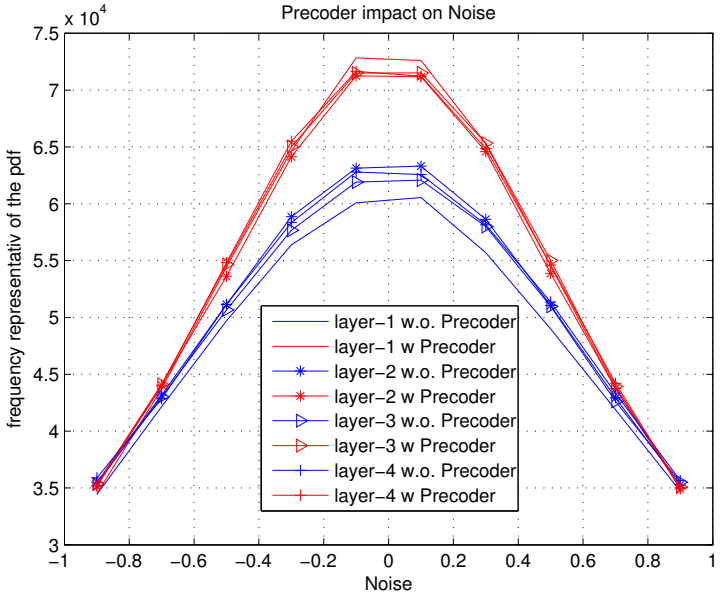

Since $\mathbf{n}$ is a vector with uncorrelated normal random variables, $\mathbf{H}^{-1}\mathbf{n}$ and $\mathbf{P}^{\mathbf{H}}\mathbf{H}^{-1}\mathbf{n}$ both represent gaussian distributions. The peak of the gaussian obtained with precoder is greater than the peak obtained by direct inversion. Since the peak is inversely proportional to the variance, it is clear that inversion without the precoder leads to noise with higher variance.

A similar simulation with SVD precoder (perfect feedback case) provides a verifiable result. The sum of noise powers are verified to be equal with and without the unitary precoder. In the SVD case, the noise variance is ordered (ascending) from layer-1 to layer-4. This is because of the convention of ordering singular values along the diagonal matrix ($\sigma_1 > \sigma_2 > \sigma_3 ...$).

Figure 5.5: Impact of Ideal SVD on Noise.Plot of frequency of occurence of noise samples(scaled pdf)

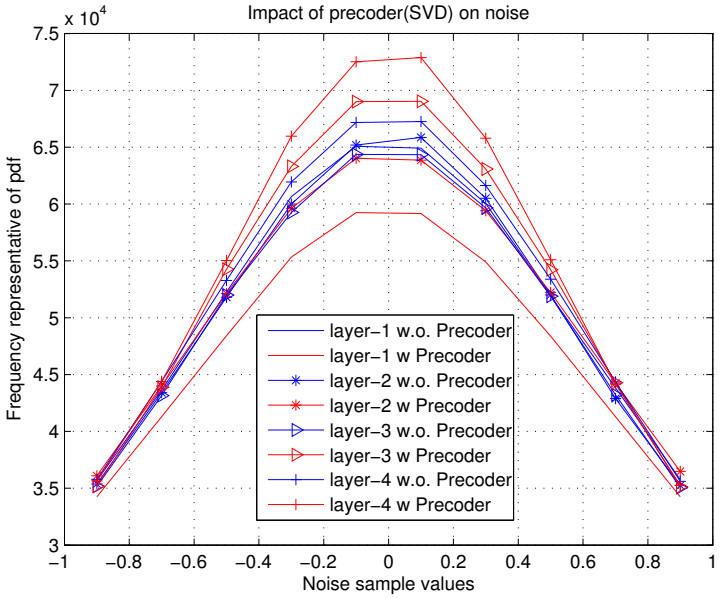

5.3 GMD in limited feedback systems

Figure 5.6: BER vs SNR, Comparison between GMD based and linear receiver under limited feedback with equal bit allocation on each stream

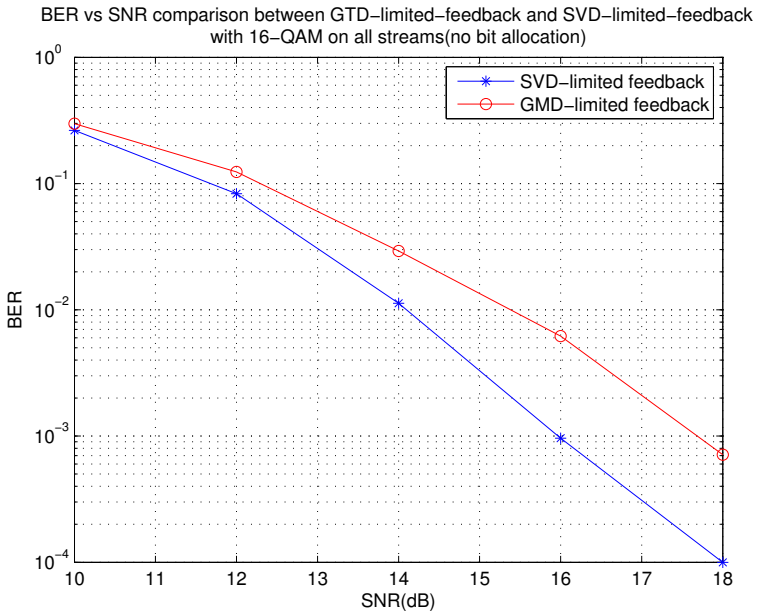

Adapting the modified SVD TRx to the GMD system, we achieve very poor results, the precoder matrix that is optimal for SVD is no longer optimal with GMD.

$$
\begin{aligned}
\mathbf{H} &= \mathbf{QRP^T} \\
\mathbf{y} &= \mathbf{GHFs} + \mathbf{Gn} \\
\mathbf{G} &= (diag(\mathbf{R}))^{-1}\mathbf{R}(\mathbf{HF})^{-1} \\
\mathbf{y} &= (diag(\mathbf{R}))^{-1}\mathbf{Rs} + \mathbf{Gn}
\end{aligned}
$$

Optimal DFE MIMO with limited feedback

We achieve better results following the model proposed in (Shenouda and Davidson, 2007). This model is the optimal limited feedback MIMO system. It can be seen from the following plot that the optimal limited feedback system is able to match the performance of the perfect feedback system. Since the diagonal elements of the triangular matrix are equal, the optimal DFE TRx may be considered as a variant of the GMD TRx.

Figure 5.7: BER vs SNR, Comparison between optimal DFE type MIMO-5×4 TRx and Linear MIMO-5×4 TRx under limited feedback using Grassman Codebook

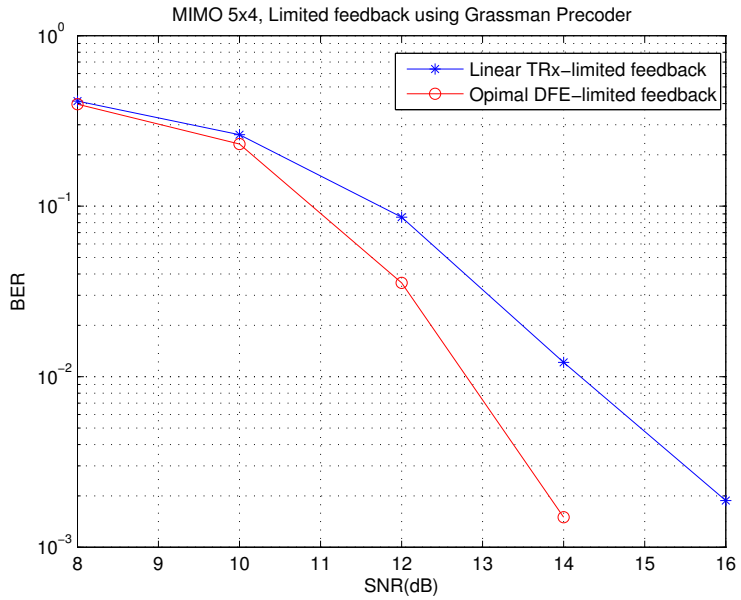

Figure 5.8: BER vs SNR, Impact of bit allocation on limited feedback systems

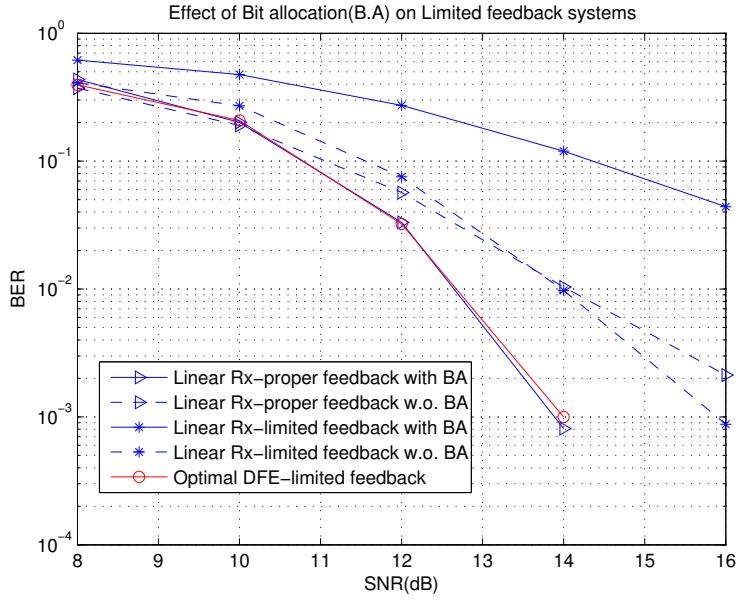

Interestingly, the bit allocation rule is no longer effective under limited feedback. Infact it degrades the performance of the limited feedback system.

5.4 Impact of bit allocation on systems with channel estimation error

One possible explanation to the degradation of BER performance with bit allocation is that under limited feedback is the uncertainty introduced by the quantization of precoder. If this is the case, similar behaviour has to be observed when channel estimation error is accounted for. It is seen from the following plots that the bit allocation scheme derived from the channel estimate achieves better results than equal bit allocation. Hence, we conclude that the quantization of precoders is not the reason for the bit allocation scheme being ineffective.

Figure 5.9: Impact of BA on systems with channel estimation error

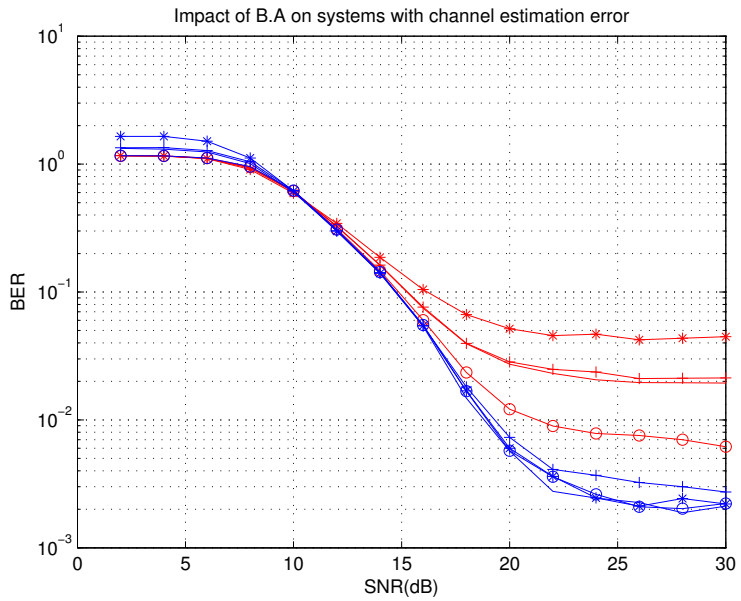

Optimal Bit allocation with limited feedback.

From derviation in Weng *et al.* (2010) we have,

$$P_{trans} = \sum_{k=1}^{M} c_k 2^{b_k} [\mathbf{F^H F}]_{kk} [\mathbf{G G^H}]_{kk} \geq M \prod_{k=1}^{M} \left(c_k 2^{b_k} [\mathbf{F^H F}]_{kk} [\mathbf{G G^H}]_{kk} \right)^{\frac{1}{M}}$$

Therefore, minimum P_{trans} is achieved when for a given $\mathbf{F}, \mathbf{G}$, each term of the

sum is equal to the geometric mean, since the geometric mean is a constant. This bit allocation scheme would be different from the scheme for an ideal feedback system in which $\mathbf{G}$ and $\mathbf{F}$ are unitary.

Using this equation to calculate the bit allocation, the following result was obtained.

Figure 5.10: Optimal Bit allocation for limited feedback Linear Receiver

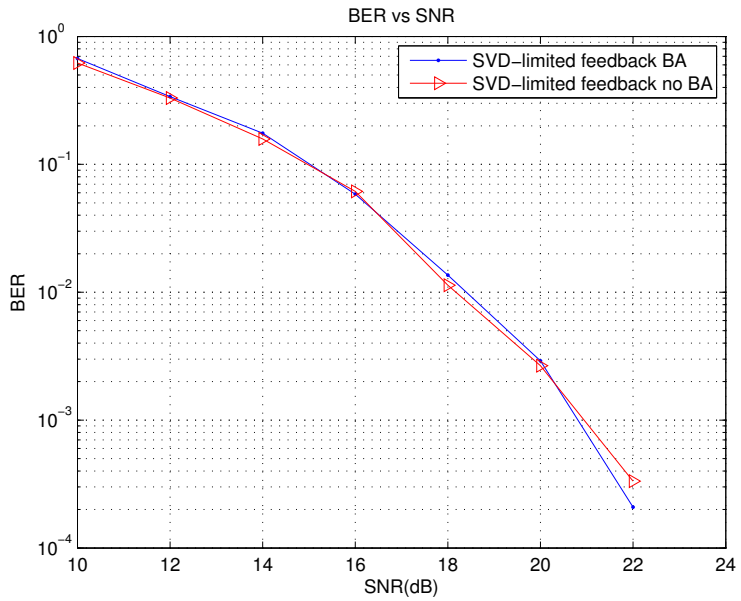

As can be seen from the result, the optimal scheme and no bit allocation schemes produce similar results. On further analysis of the simulation, it was seen that the optimal scheme was more or less close to equal bit allocation. Thus, under limited feedback scenarios the computing bit allocation is unneccesary.

5.5 Reduction of computational complexity

The problem of deriving a grassman codebook is highly non-trivial. However, we hypothesize that if a grassman codebook is available, then close to optimal codebooks of smaller sizes can be easily derived from it.

As mentioned in section-4.1.1 in the report, grassman codebook represents the solution to the max-min problem.

$$\max\min d(\mathbf{P_k}, \mathbf{P_i}) = |\mathbf{P_k}\mathbf{P_k^H} - \mathbf{P_i}\mathbf{P_i^H}|_\mathbf{2} \quad i = 1, 2..256, j = 1, 2..256$$
$$Such\ that \qquad P_i, P_k \in \mathcal{U}(5, 4)$$

$\mathbf{P_i}$s are all maximally spaced matrices, let the codebook be represented by $\mathcal{C}$. Now If we were to solve for a codebook with 2 matrices $(\mathbf{P_1^{'}}, \mathbf{P_2^{'}})$ as follows,

$$\max\min d(\mathbf{P_1^{'}}, \mathbf{P_2^{'}}) where\ P_1^{'}, P_2^{'} \in \mathcal{C}$$

This would be same as finding 2 matrices that are farthest apart. Let this codebook be refered to as $\mathcal{C}_2^{'}$. We propose a method where in we construct a n+1 size codebook, as $\mathcal{C}_{n+1}^{'} = \mathcal{C}_n^{'} \cup \{P_{n+1}^{'}\}$ where $P_{n+1}^{'}$ is given by the solution of $d(\mathbf{P_{n+1}^{'}}, \mathcal{C}_n^{'}) = \max d(\mathbf{P}_i^{'}, \mathcal{C}_n^{'})\ \forall \mathbf{P_i^{'}} \in \mathcal{C} - \mathcal{C}_n^{'}$. The codebook $\mathcal{C}_{n+1}^{'} = \mathcal{C}_n^{'} \cup \{\mathbf{P_{n+1}^{'}}\}$ is not optimal, however, even this suboptimal codebook is seen to give close to optimal results with as low as 4 precoders.

Figure 5.11: Impact of Grassman Codebook simplification, BERvsSNR comparison between Limited feedback Linear MIMO(5×4) TRx using grassman codebook of size 256 and reduced codebook of size 4

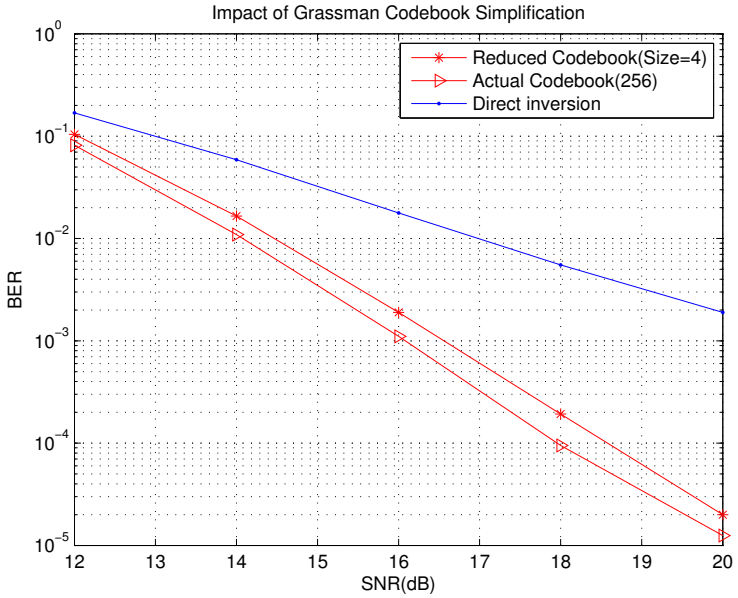

Hence, if the channel permits the use of smaller size codebooks then it will reduce the computational complexity on the reciever side and also valuable number of feedback

bits could be saved.

If the channel is highly uncorrelated then we observe that channel inversion works well. Since the reduced codebook does not have the identity matrix its performance is poorer compared to channel inversion.

Figure 5.12: Impact of Grassman Codebook simplification, BER vs SNR comparison between Limited feedback Linear MIMO(5×4) TRx using grassman codebook of size 256 and reduced codebook of size 4 when channel is uncorrelated channel

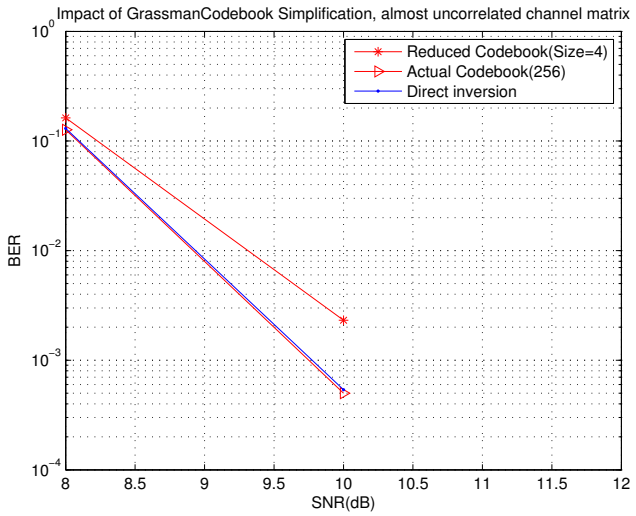

Figure 5.13: Impact of Grassman Codebook simplification, BERvsSNR comparison between Limited feedback Linear MIMO(5×4) TRx using grassman codebook of size 256 and reduced codebook of size 4, in the presence of channel estimation error($\mathcal{N}(0, 0.1)$

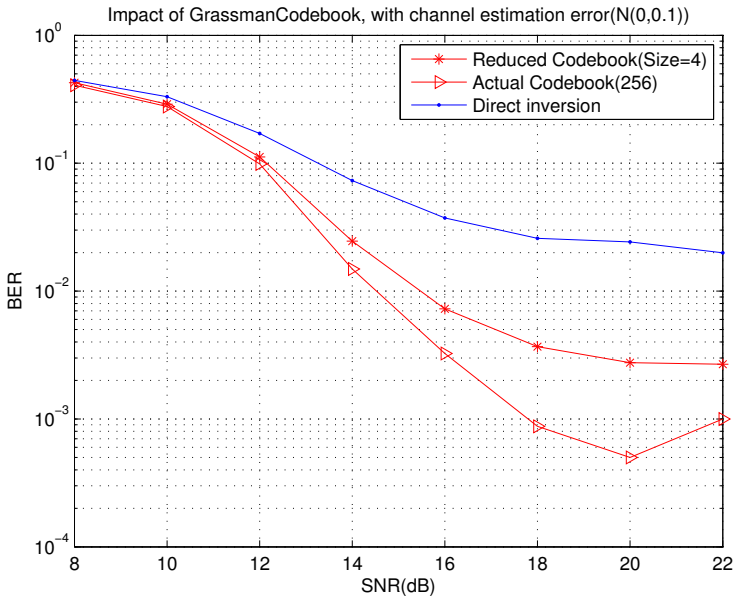

Figure 5.14: Impact of Grassman Codebook simplification Limited feedback DFE

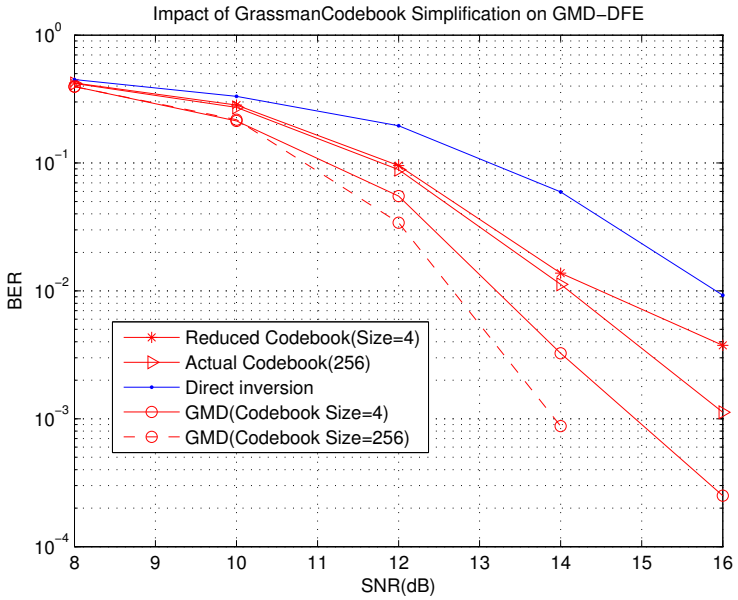

CHAPTER 6

Masking channel estimation errors by Quantization Noise

In the previous section, we had proposed a codebook reduction algorithm which maybe used when the channel is good i.e. it allows for the use of fewer precoder matrices while still achieving the required performance. An alternate case in which the quantization noise might not affect the performance would be the presence of high channel estimation error. Though it has been assumed that complete CSIT is present, it is often not possible to accurately estimate the channel matrix $\mathbf{H}$, hence it is neccesary to account for the same.

If the channel estimate given by $\mathbf{H}$ is erroneous such that the actual channel is given by $\mathbf{H} + \triangle\mathbf{H}$, where $\triangle\mathbf{H}$ is the estimation error then, we model the estimation error such that each element is a gaussian perturbation $\mathcal{N}(0, \sigma_{err}^2)$.

$$\mathbf{E}[|\triangle\mathbf{H}_{ij}|] = \frac{2\sigma_{err}}{\sqrt{2\pi}} \int_0^{\inf} xe^{-\frac{x^2}{2}} dx = \frac{2\sigma_{err}}{\sqrt{2\pi}} \int_0^{\inf} e^{-z} dz = \sqrt{\frac{2\sigma_{err}^2}{\pi}}$$

$$\frac{\mathbf{E}[|\triangle\mathbf{H_{ij}}|]}{\mathbf{E}[|\mathbf{H_{ij}}|]} = \sigma_{err}$$

Hence, σ_{err} indicates the percentage error in the estimate. Suppose we are trying to transmit 4 bits of data, but it is also known that the last 2 bits are badly affected by noise that they might as well be randomly generated at the receiver. In such a scenario, reducing the quantization levels from 2^4 to 2^2 will not degrade the performance. Similarly, if there is channel estimation error, then the optimal precoder matrix cannot be accurately obtained, this deviation from the accurate precoder might be masked by reducing the codebook size which will help in saving a few precious feedback bits and reduce computation (comparisons) on the receiver side.

Figure 6.1: Quantization masking channel estimation error. BER vs SNR comparison between linear MIMO TRx using codebooks of size 256 and size 4 under various channel estimation error levels.

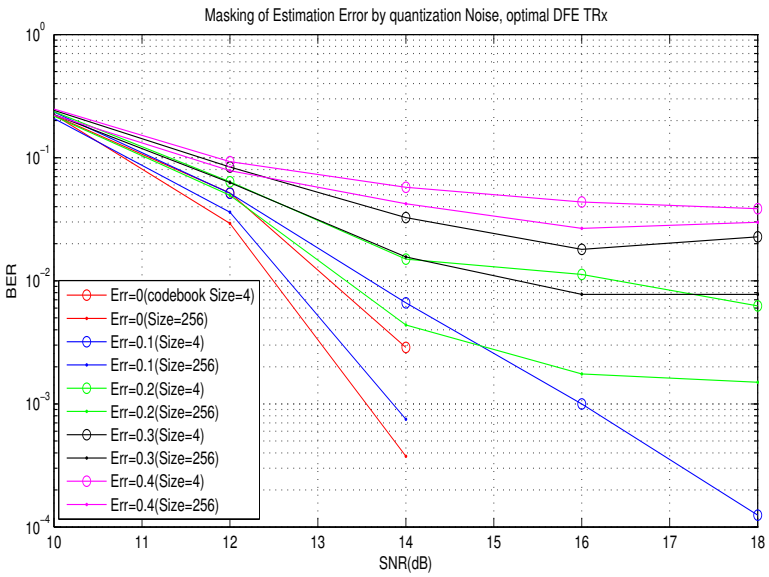

We observe from the above plot that masking of channel estimation errors by quantization noise would not be fruitful since the masking becomes effective only under very high channel estimation errors.

CHAPTER 7

Conclusion and Future work

Conclusion

Various MIMO limited feedback systems were studied. Firstly, the performance improvement provided by GTD tends to be negligible and in the case of limited feedback systems, GTD does not provide any additional value. Also the quantization noise present in the limited feedback cases can be avoided by introducing a non-linear inversion operation at the receiver. It has also been observed that choosing the optimal precoder leads to a conditioning effect on noise which results in better BER values.

Grassman codebooks were studied and an efficient sub-optimal algorithm to reduce a code book from larger size was introduced. Under the chosen channel conditions the smaller codebooks performed close to the baseline case. Hence, it can be used to reduce computational complexity and feedback.

The idea of masking channel estimation noise by quantization noise does not seem feasible, as the estimation error has to be very high for it to be effective.

If we were to make suggestions to current LTE spatial mutliplexing standards based on the studies performed, we would suggest the following- use of a GMD based optimal DFE transceiver instead of the linear transceiver will help achieve performance close to the ideal CSIT scenario. Also, use of a flexible codebook as hypothesized earlier could help save valuable feedback bits and also reduce the computations required. Suppose the channel is very good, the system should be able to achieve the required BER values with a smaller codebook size. A smaller codebook size would mean fewer feedback bits and fewer comparisons while choosing the optimal algorithm. And the proposed induction based algorithm of codebook reduction would imply that the system could use one master codebook stored in the memory and the reduced codebooks could simply be the subsets of master codebook, and the codebook can be designed such that the reduced codebook of size n would simply be the first n matrices of the master codebook.

Problems to explore

- Obtaining a bit allocation formula under improper channel estimation.
- Establishing the underlying structure of the matrices in the grassman subspace to verify level of deviation of the optimal codebook from the reduced codebook that has been proposed.
- Theoretical explanation as to why the inversion with the precoder works as well as it does.
- Possibly employ vector decision as the noise is correlated across the streams.
- Analysis of the TRx schemes have been done on ZF type receivers, similar analysis maybe done on MMSE type receivers.

APPENDIX A

LTE MIMO modes

Table A.1: LTE MIMO modes

#	Mode	Description
1	Single Antenna Mode(Port 0)	1 data stream is transmitted using a single antenna, while there may be one or more receive antennas(receiver diversity)
2	Transmit Diversity	This involves the transmission of the same stream over multiple transmit antennas.
3	Open loop-Spatial Multiplexing	2 data streams are transmitted over 2 or more(upto 4) transmit antennas. There is no feedback though the TRI(transmit rank indicator) is available at the base station to select the number of levels.
4	Closed loop-Spatial Multiplexing	Similar to the open loop case, but the PMI(precoding matrix indicator) is also fedback to the transmitter.
5	Multi-user MIMO	Difference from Closed loop spatial multplexing is that the data streams are targetted towards different users.
6	Closed Loop Rank 1 with precoding	One code word is transmitted over one spatial layer, it is similar to beamforming
7	Single Antenna(Port 5)	This is a beamforming mode, 1 stream over 1 spatial layer. 1-4 antennas.

REFERENCES

1. **D.Love** (). Tables of complex grassmannian packings[online].

2. **Frenger-EricsonResearch** (2009). Mimo in lte and lte-advanced.

3. **Goldsmith, A.**, *Wireless communications*. Cambridge university press, 2005.

4. **Jiang, Y.**, **W. Hager**, and **J. Li** (2008). The generalized triangular decomposition. *Mathematics of computation*, **77**(262), 1037–1056.

5. **Jiang, Y.**, **J. Li**, and **W. W. Hager** (2005*a*). Joint transceiver design for mimo communications using geometric mean decomposition. *Signal Processing, IEEE Transactions on*, **53**(10), 3791–3803.

6. **Jiang, Y.**, **J. Li**, and **W. W. Hager** (2005*b*). Uniform channel decomposition for mimo communications. *Signal Processing, IEEE Transactions on*, **53**(11), 4283–4294.

7. **Lin, Y.-P.** and **S.-M. Phoong** (2001). Optimal isi-free dmt transceivers for distorted channels with colored noise. *Signal Processing, IEEE Transactions on*, **49**(11), 2702–2712.

8. **Love, D. J.** and **R. W. Heath** (2005). Limited feedback unitary precoding for spatial multiplexing systems. *Information theory, IEEE Transactions on*, **51**(8), 2967–2976.

9. **Mietzner, J.**, **R. Schober**, **L. Lampe**, **W. H. Gerstacker**, and **P. A. Hoeher** (2009). Multiple-antenna techniques for wireless communications-a comprehensive literature survey. *Communications Surveys & Tutorials, IEEE*, **11**(2), 87–105.

10. **Schwarz, S.**, **C. Mehlfuhrer**, and **M. Rupp**, Calculation of the spatial preprocessing and link adaption feedback for 3gpp umts/lte. *In Wireless Advanced (WiAD), 2010 6th Conference on*. IEEE, 2010.

11. **Shenouda, M. B.** and **T. N. Davidson**, Limited feedback design of mimo systems with zero-forcing dfe using grassmann codebooks. *In Information Theory, 2007. CWIT'07. 10th Canadian Workshop on*. IEEE, 2007.

12. **Telatar, E.** (1999). Capacity of multi-antenna gaussian channels. *European transactions on telecommunications*, **10**(6), 585–595.

13. **TelesystemInnovations** (2009). The seven modes of mimo in lte.

14. **Tse, D.**, *Fundamentals of wireless communication*. Cambridge university press, 2005.

15. **Weng, C.-C.**, **C.-Y. Chen**, and **P. Vaidyanathan** (2010). Mimo transceivers with decision feedback and bit loading: theory and optimization. *Signal Processing, IEEE Transactions on*, **58**(3), 1334–1346.

16. **Wolniansky, P. W.**, **G. J. Foschini**, **G. Golden**, and **R. Valenzuela**, V-blast: An architecture for realizing very high data rates over the rich-scattering wireless channel. *In Signals, Systems, and Electronics, 1998. ISSSE 98. 1998 URSI International Symposium on*. IEEE, 1998.